Article

Construction of plasmonic core-satellite nanostructures on substrates based on DNA-directed self-assembly as a sensitive and reproducible biosensor

Tingting Zhang, He Li, Shengwei Hou, Youqing Dong, Guangsheng Pang, and Yingwei Zhang

ACS Appl. Mater. Interfaces, **Just Accepted Manuscript** • DOI: 10.1021/acsami.5b07152 • Publication Date (Web): 19 Nov 2015

Construction of plasmonic core-satellite nanostructures on substrates based on DNA-directed self-assembly as a sensitive and reproducible biosensor

Tingting Zhang,[†] He Li,[†] Shengwei Hou,[†] Youqing Dong,[§] Guangsheng Pang,[‡] and Yingwei Zhang[*†]*

[†] State Key Laboratory of Chemical Resource Engineering & Key Laboratory of Carbon Fiber and Functional Polymers, Ministry of Education; College of Materials Science & Engineering, Beijing University of Chemical Technology, Beijing, 100029, China

[‡] State Key Laboratory of Inorganic Synthesis and Preparative Chemistry, College of Chemistry, Jilin University, Changchun, 130012, China

[§]College of Chemistry and Materials Engineering, Wenzhou University, Wenzhou, 325027, China

Abstract

We report the successful construction of plasmonic core-satellite nanostructured assemblies on two-dimensional substrates, based on a strategy of combining DNA-functionalized plasmonic

nanoparticles (NPs) with the specific recognition ability toward target to enable satellite NPs to self-assemble around the core immobilized on substrates. A strongly coupled plasmonic resonance band was observed due to the close proximity between core and satellite NPs, which presented significant red-shift and enhanced extinction with respect to the local surface plasmon resonance (LSPR) band of individual core NPs on the substrate. The functionality of this core-satellite nanostructured assembly as a biosensor was further explored, and the changes in extinction intensity and the peak shift of the plasmonic coupling resonance band arising from the probe-target DNA binding event all proved to be useful criteria for target DNA detection. Moreover, high selectivity down to single-base mismatched DNA was achieved using this strongly coupled plasmonic core-satellite nanostructured assembly on a substrate. Such substrate-based detection was advantageous, and its reusability and high cycle stability were demonstrated after five cycles of disassembly and reassembly. Our work demonstrates the biosensing capacity of this DNA-functionalized plasmonic nanoassembly model system on two-dimensional substrate, which is also applicable to the detection of numerous DNA-recognized biomolecules. Likewise, the presented construction method can be extended to fabricate other compositional core-satellite nanoassemblies.

Keywords:

Local surface plasmon resonance, Plasmon coupling, core-satellite nanostructure, self-assembly, biosensor, reproducibility

Introduction

Biosensors based on the specific recognition capacity of DNA probe towards target biomolecules have attracted the extensive attention of scientists in various research areas for their high selectivity, sensitivity and structure switchable sensing ability toward multiple types of target analytes.[1] Nevertheless, probe-target binding event in these biosensors only serve as the biorecognition element, one of the two components required by a sensing device, and thus nanomaterials with unique optical, electronic and magnetic properties are integrated into the fabrication of biosensors to serve as a signal transducer element to transform the recognition event into a measurable output signal.[2,3] Among these signal transduction methods, nanomaterial-based fluorescent biosensors have been widely developed for the detection of DNA, protein and metal ions,[4-6] and we together with some other researchers have carried out some related work in this field.[7-9] However, fluorescent biosensors usually suffer from disadvantages such as limited fluorescence lifetime and photobleaching of the fluorophore, which have become the bottlenecks to further practical applicationa.[10]

Plasmonic nanoparticles (NPs) such as Au NPs and Ag NPs, possess unique optical properties arising from local surface plasmon resonance (LSPR), which results from the resonant interaction of incident light with the collective oscillation of conduction electrons confined to a nanoscale volume; these materials have important applications in various research areas including LSPR sensing.[11-13] It is known that such plasmon resonance is sensitive to the size, shape, composition and dielectric medium surrounding NPs.[14,15] In addition, surface plasmons can be coupled when two or more discrete plasmonic NPs are brought into close proximity to form aggregates or assemblies, leading to new resonance bands in the optical spectrum due to the interaction of their oscillating electric fields.[16-18] Based on the abovementioned factors,

plasmonic-based biosensors have therefore been constructed by monitoring the resonance peak shift as a result of the target molecule binding event to perform detection. Compared with fluorescence biosensors, plasmonic-based biosensors present more advantages in terms of photostability and biocompatibility, and besides, plasmonic NPs are ~500,000 times more luminous than fluorophores, which provides greater sensitivity.[19] Because the LSPR absorption bands of Au NPs and Ag NPs are within the visible spectrum region, a color change due to the combination of target analytes can be observed with the naked eye, and consequently colorimetric naked-eye sensors have been extensively explored and utilized as powerful diagnostic platforms for the detection of a range of biomolecules,[20,21] heavy metal ions[22,23] and small molecules,[24-26] since the pioneering work of Mirkin and Alivisatos *et al*.[27,28] However, it should be mentioned first that the plasmonic-based biosensors are mostly based on the aggregation of NPs in a colloidal solution, and there are some unavoidable and undesirable occurrences in solution-based detecting methods, such as aggregation of nanoparticles caused by pH, temperature and salt concentration, leading to a subsequent false positive signal readout.[19,29] In order to solve this problem, transferring NPs from solution to a solid substrate is a good alternative. Furthermore, another issue that should be addressed is how to control and enhance plasmonic coupling to increase the sensitivity of plasmonic biosensors, since the plasmonic coupling which is used to detecting the probe-target recognition event usually arises from the aggregation of NPs.

The self-assembly strategy provides a fascinating approach to control and enhance the plasmonic properties of nanostructures, and the construction of self-assembled nanostructures on a two-dimensional substrate can minimize undesirable NPs aggregation that occurs in solution-based methods.[19,29,30] Based on this, we considered combining a self-assembly strategy and a

plasmonic-based biosensor, by applying DNA-functionalized plasmonic NPs with single-sized substrate-immobilized plasmonic NPs as the core and another size of plasmonic NPs as the satellites to construct a core-satellite nanostructured assembly on a two-dimensional substrate through the specific binding of the probe DNA and the target. The core-satellite nanostructure is an excellent example of strongly coupled plasmon assemblies, and has raised considerable interest in areas including plasmon ruler and surface enhanced Raman scattering.[30,31] Here, we utilized a core-satellite nanostructure on a two-dimensional substrate as a controllable and enhanced plasmonic nanostructure for the self-assembly of foreign plasmonic satellite NPs around a core immobilized on the substrate in advance. We expected this to lead to an obviously enhanced plasmonic coupling resonance shift relative to the individual core NPs and reversible recovery to the original individual core structure upon disassembly due to the immobilization of the core on the substrate, accompanied by the disappearance of the plasmonic coupling resonance band. Hence, a controllable strongly coupled plasmonic nanostructure on a two-dimensional substrate with reproducible detection ability based on disassembly and subsequent reassembly was the aim of our design.

As a proof of concept to demonstrate the biosensing functionality and reusability of a plasmonic core-satellite nanostructured assembly on a two-dimensional substrate, we utilized DNA probe functionalized Au NPs with different sizes as the cores and satellites, and chose complementary DNA with its reversible hybridization ability as the model target of detection and a linker for self-assembly. In the present research, we first investigated the effect of core size on the self-assembled core-satellite nanostructure, confirming that a plasmonic core-satellite nanostructured assembly composed of 40 nm diameter Au NPs as the core and 17 nm diameter Au NPs as the satellites produced a stronger plasmonic coupling resonance response compared to

other sizes of core-satellite nanostructured assemblies. Then, we studied the sensing ability of this assembled structure toward complementary target DNA, and found that changes in the extinction intensity of the plasmonic coupling resonance peak as well as the peak shift with an increasing target DNA concentration were related to the assembled numbers of satellites surrounding core NPs. Additionally, the differentiation of single-base mismatched DNA could be performed based on this assembled nanostructure. The reusability of this substrate-based assembly as a biosensor was demonstrated after five cycles of disassembly and reassembly with high cycle stability.

Experimental Section:

Reagents and materials:

$HAuCl_4 \cdot 4H_2O$ was obtained from Sinopharm Chemical Reagent Co., Ltd. All chemically synthesized oligonucleotides were purchased from Sangon Biotech. Co. Ltd. (Shanghai, China). Tris(2-carboxyethy1)phosphine (TCEP), bis(p-sulfonatophenyl)phenylphosphine (BSPP), (3-aminopropyl)triethoxysilane (APTES), sulfosuccinimidyl-4-[N-maleimidomethyl]cyclohexane-1-carboxylate (sulfo-SMCC) and Tris(hydroxymethyl)aminomethane (Tris) were purchased from Sigma-Aldrich. All the other chemicals were purchased from Beijing Chemical Reagent Co., Ltd. All chemicals were used without further purification and the water used throughout all experiments was purified using a Millipore system. The buffer solutions used in all the experiments were prepared as follows: PB buffer (10 mM Na_2HPO_4/NaH_2PO_4, pH=7.4), TE buffer (40 mM Tris, 2 mM EDTA, pH=7.4), 0.5×TBE buffer (89 mM Tris, 89 mM boric acid, 2 mM EDTA; pH=8.0), 1×TAE/Mg^{2+} buffer (40 mM Tris, 20 mM acetic acid, 2 mM EDTA and 12.5 mM magnesium acetate; pH=8.0).

The DNA oligonucleotides were purchased from Shanghai Sangon Biotechnology Co. Ltd. (Shanghai, China). Oligonucleotides sequences are listed as follows (mismatches are underlined, perfectly matched sequences are highlighted in bold):

(1) P_1: (probe DNA modified on the surface of core NPs with a segmental sequence as the capture strand to hybridize target DNA and T_{15} as the spacer sequence)

5'-**AAT ACT GCG ACT AAT**- T_{15}-C_6H_{12}-SH-3'

(2) P_2: (probe DNA modified on the surface of satellite NPs with a segmental sequence as the capture strand to hybridize target DNA and T_{15} as the spacer sequence)

5'-HS- C_6H_{12}-T_{15}- **TTA TGA CCC TGA TTA**-3'

(3) T_0: (target DNA which complementary to probe DNA P_1 and P_2 as the linker for core-satellite assembly)

5'-**ATT AGT CGC AGT ATT TAA TCA GGG TCA TAA**-3'

(4) T_1: (single-base mismatched target)

5'-ATT AGT CGC AGT ATG TAA TCA GGG TCA TAA-3'

(5) T_2: (two-base mismatched target)

5'-ATT AGT CGC AGT ATG TCA TCA GGG TCA TAA-3'

(6) T_3: (three-base mismatched target)

5'-ATT AGT CGC CGT ATG TCA TCA GGG TCA TAA-3'

(7) T_n: (non-complementary target)

5'-TTT TTT TTT TTT TTT TTT TTT TTT TTT TTT-3'

(8) T_L: (a long strand with middle domain containing complementary target)

5'-TTT TTT TTT TTT TTT TTT TTT **ATT AGT CGC AGT ATT TAA TCA GGG TCA TAA** TTT TTT TTT TTT TTT TTT TTT-3'

Synthesis of different sized citrate-stabilized Au NPs

17 nm satellite NPs were prepared based on a modified Fren's method.[33-35] Sodium citrate aqueous solution (150 mL, 0.97 mM) was brought to boiling, followed by the addition of an $HAuCl_4$ (1.5 mL, 25 mM) aqueous solution under vigorous stirring. A color change was observed form yellowish to light purple and then to red. The solution was heated for a further 10 min and then cooled down slowly to room temperature.

40 nm core NPs were synthesized using a seeded growth method.[36] Firstly, sodium citrate aqueous solution (150 mL, 2.2 mM) was brought to boiling in a 250 mL three-necked round-bottom flask, then $HAuCl_4$ (1 mL, 25 mM) was injected immediately under vigorous stirring. After 15 min, the solution was cooled slowly to 90^{o}C and at this moment the resulting NPs were used as seeds. Subsequently, sodium citrate (1 mL, 60 mM) and $HAuCl_4$ solution (1 mL, 25mM) were injected into the abovementioned seed solution. Then, AuNPs 30 nm in diameter were obtained after 30 min of reaction at 90^{o}C. On the basis of 30 nm diameter AuNPs, 40 nm diameter AuNPs were prepared by repeating the previous addition of sodium citrate (1 mL, 60 mM) and $HAuCl_4$ solution (1 mL, 25 mM) and continuing the heating reaction for 30 min at 90^{o}C.

These samples were characterized by transmission electron microscopy (TEM) and UV-vis spectroscopy. The resulting AuNP colloidal solution was stored at 4^{o}C and the concentration was calculated based on the Beer-Lambert law from the absorbance value measured by UV-vis spectroscopy. The molar extinction coefficients for each AuNPs size are given as follows: 17 nm AuNPs: $\varepsilon=2.7\times10^{8}\ M^{-1}cm^{-1}$; 30 nm AuNPs: $\varepsilon=3\times10^{8}\ M^{-1}cm^{-1}$; 40 nm AuNPs: $\varepsilon=3.7\times10^{9}\ M^{-1}cm^{-1}$ [37,38].

Preparation of DNA-modified core and satellite NPs

Before the procedure of DNA modification, 3 mg BSPP was added into 10 mL as-prepared AuNPs solution under stirring to replace the citrate capping on the surface of NPs and enhance the stability of NPs.[39] After overnight incubation at room temperature, the mixture was centrifuged for 20 min (17 nm AuNPs: 1300 rpm, 40 nm AuNPs: 10000 rpm) and the AuNPs were redispersed in 1 mL of 2.5 mM BSPP solution for subsequent treatment.

In order to reduce the disulfide bonds, thiol-modified oligonucleotides (100 μM, 10 μL) were treated using TCEP (20 mM, 40μL) in TE buffer for 1 h and then purified by size exclusion columns (G-25, GE Healthcare) to remove small molecules.[39] A given volume of 100 μM DNA solution (20 μL P_1 for core NPs and 10 μL P_2 for satellite NPs) was added into 1 mL 0.5×TBE buffer containing core or satellite NPs and incubated for 12 h at room temperature. Then, in order to enhance the binding of thiolated DNA on the surface of NPs, the concentration of NaCl in this system was gradually increased to 300 mM with a 50 mM change in each step every 8 hours. Then, the as-prepared DNA-modified NPs were washed three times with 0.5×TBE buffer to remove the extra free oligonucleotides. At last, 40 nm DNA-modified core NPs were redispersed in ultrapure water ([Au NPs] ≈ 0.4 nM), while 17 nm DNA-modified satellite NPs were redispersed in 1×TAE/Mg^{2+} buffer with 0.05%SDS ([Au NPs] ≈ 5 nM).

Immobilization of core NPs on the surface of substrates:

First, the silicon or quartz (11 mm×12 mm) substrate was cleaned by immersing it in piranha solution (H_2SO_4:H_2O_2=7:3) for 1 h, washed thoroughly with ultrapure water and dried under N_2 flow. The cleaned substrate was immersed into a toluene solution of APTES ($1x10^{-5}$ M) for 8 h,

washed with toluene, acetone and ethanol in sequence for three times, dried under N_2 flow and baked at 110°C for 15 min; thus, a monolayer of amino groups on the surface was obtained.

In order to immobilize core NPs on the substrate, 120 μL of as-prepared DNA-modified core NPs solution was spread onto the amino group functionalized substrate and incubated for 2 h under humid conditions. Driven by electrostatic interactions, negatively charged core NPs were immobilized on the surface of the positively charged substrate in this procedure. Then, the substrate was washed three times with distilled water and dried under N_2 flow.

Fabrication of core-satellite nanostructured assembly via DNA hybridization on substrate

Before the assembly procedure, to avoid non-specific adsorption of the satellite NPs, the core-immobilized substrate was immersed in 1 mL of 0.01 M PB buffer containing sulfo-SMCC (2 mM) at 45°C for 2 h to neutralize the residual surface charges provided by extra amino groups, followed by washing and drying. In the following core-satellite assembly process, single strand target DNA T_0, which is completely complementary to the DNA capture strands P_1 and P_2 on the core and satellite NPs, respectively, was first introduced to the substrate as a linker between core and satellite NPs for subsequent assembly. More specifically, the capture strand P_1 capping core-immobilized substrate was immersed in 1 mL of 1xTAE/Mg^{2+} buffer containing different concentrations of target DNA T_0 for hybridization, incubated at 65°C for 5 min and then allowed to anneal slowly at room temperature for 8 h, after which the substrate was taken out and washed with distilled water three times to remove unhybridized target DNA T_0, and dried under N_2 flow. Then, 120 μL of capture strand P_2 modified satellite NPs was added to hybridize to the unhybridized part of the target DNA T_0 bound to the core NPs of the substrate; this was then

incubated at 45°C for 5 min and annealed slowly at room temperature for 2 h, followed by washing to remove unbound NPs and drying.

Disassembly of the core-satellite nanostructure to obtain a reproducible substrate for subsequent reassembly

An assembled core-satellite substrate was immersed in distilled water and heated at 90°C for 5 min, which is above the melting temperature, taken out and quickly dipped into a mixture of ice and water for quenching and dehybridization, followed by thorough washing with distilled water. After the abovementioned disassembly procedure, the satellite NPs were released due to the dehybridization of DNA capture strands with target strands and washed away while the core NPs were reserved because of their electrostatic interaction with the substrate. For a reproducible core substrate, satellite NPs were reassembled according to the previous procedure and cycle stability was assessed based on the results of five cycles of assembly and disassembly.

Characterization:

Scanning electron microscopy (Zeiss EVO MA25) was used to characterize the core-satellite nanostructures with silicon as the supporting substrate. The UV-vis spectra were measured using a Hitachi U-3900H spectrophotometer, with quartz slides as the supporting substrate. Transmission electron microscopy (H-800, Hitachi) was used to characterize as-prepared Au NPs.

Results and discussion

In order to construct plasmonic core-satellite nanostructures on the substrate, we utilized a self-assembly strategy as illustrated in Scheme 1. In general, this self-assembly strategy includes four steps: (a) functionalization of the substrate with APTES to obtain a positively charged amino-terminated surface; (b) immobilization of capture strand DNA-modified core NPs on the substrate based on electrostatic interactions; (c) introducing sulfo-SMCC to shield the extra positive charge of the substrate by the formation of covalent bonds with amino groups (d) assembly of satellite NPs decorated with another capture strand around core NPs via hybridization between the target DNA and the two capture DNA strands. After the accomplishment of the self-assembly process, it was anticipated that there would be obvious changes in the optical spectrum and color due to strong surface plasmon coupling between core and satellite NPs arising from the formation of the core-satellite nanostructured assembly.

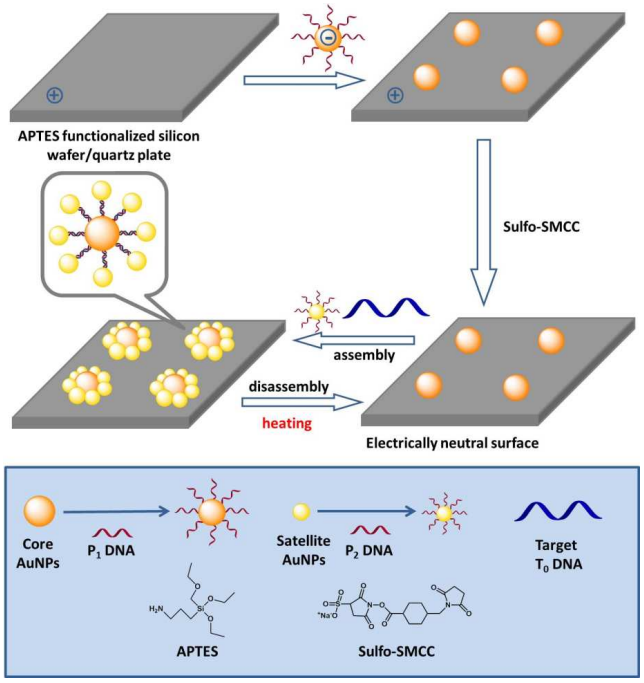

Scheme 1. A schematic (not to scale) illustration of the self-assembly procedure for the construction of a plasmonic core-satellite nanostructure.

Before the assembly process, different sized Au NPs with average diameters of 17 nm, 30 nm and 40 nm were fabricated using a method combining citrate reduction and seeded growth. As shown in the TEM photograph of Figure S1, the as-prepared Au NPs were all monodispersed with a spherical shape and uniform size distribution. The UV-vis spectra of different sized Au NP aqueous solutions were measured as shown in Figure S1, showing that the 40 nm NPs had an SPR maximum at 528 nm, while 30 nm NPs had a SPR maximum at 523 nm and 17 nm NPs had a SPR maximum at 519 nm. Subsequently, these Au NPs (17 nm, 30 nm and 40 nm) were all functionalized with the thiol-modified single strand probe DNA (ssDNA), and the concentration of ssDNA-modified NPs was determined using UV-vis spectrum. Then, we utilized fixed-sized satellite NPs 17 nm in diameter around different sized core NPs (17 nm, 30 nm and 40 nm in diameter) to assemble core-satellite nanostructures in the presence of target DNA at 100 nM, to investigate the effect of core size on the assembly of the core-satellite nanostructure. It should be noted that the extinction peak position of core NPs immobilized on the quartz substrate was a little different from that measured in colloidal solution, as a slight shift and broadening of the plasmon band was observed, which may be attributed to changes in interparticle distance as well as the dielectric medium surrounding core NPs.[40,41] Then, we found that a new resonance band indeed appeared as expected in the UV-vis spectra after the self-assembly of the core-satellite nanostructure on the quartz substrate, which was ascribed to the inter-particle plasmonic coupling between core and satellite NPs as a result of the probe-target binding event,[18] which differed from the LSPR bands of the individual core and satellite NPs. With increasing size of the core NPs, the new plasmonic resonance peak was red-shifted and complete core-satellite nanostructured assemblies were gradually formed, as characterized by UV-vis spectra and SEM,

which are shown in Figure S2 and Figure 1. As presented in Figure 1a, the plasmonic core-satellite nanostructured assembly consisting of 40 nm diameter Au NPs as cores and 17 nm diameter Au NPs as satellites showed the largest red-shift of 61 nm, compared to the newly formed plasmonic coupling resonance band caused by self-assembly with the LSPR band of individual core NPs on the substrate. It is a reasonable result that plasmonic coupling resonance peak wavelength is shifted to larger values with increasing size of plasmonic core NPs, due to enhanced dipole-dipole interactions when increasing the particle size, leading to enhanced plasmonic coupling between core and satellite NPs.[42-44] And at the same time, cores of greater size can accommodate more satellite NPs, which is also accountable for core size-dependent plasmonic optical property in the abovementioned results. It should be mentioned that the newly-formed plasmonic resonance band in UV-vis spectra should be composed of the transverse coupling located near the SPR band of the isolated Au NPs, and the longitudinal coupling of the surface plasmons which contribute to the red-shift of plasmonic resonance band.[45,46] When the core-satellite nanostructure is completely assembled, owning to the smaller distance between transverse and longitudinal coupling resonance peak arising from relatively larger distance between core and satellite NPs based on the fixed base number, transverse and longitudinal coupling cannot be obviously differentiated from each other and consequently formed an overlap peak in plasmonic resonance band. The difference in the UV-vis spectra before and after self-assembly was also visible to the naked eye, as shown in the optical images in the inset of Figure 1a, and the morphological changes shown in SEM the images, showing that the 17 nm Au satellite NPs around 40 nm Au core NPs formed an almost coplanar core-satellite nanostructured assembly. This interesting coplanar configuration had also been observed in other studies, and

the phenomenon is probably the result of capillary forces between satellite NPs and the substrate.[30]

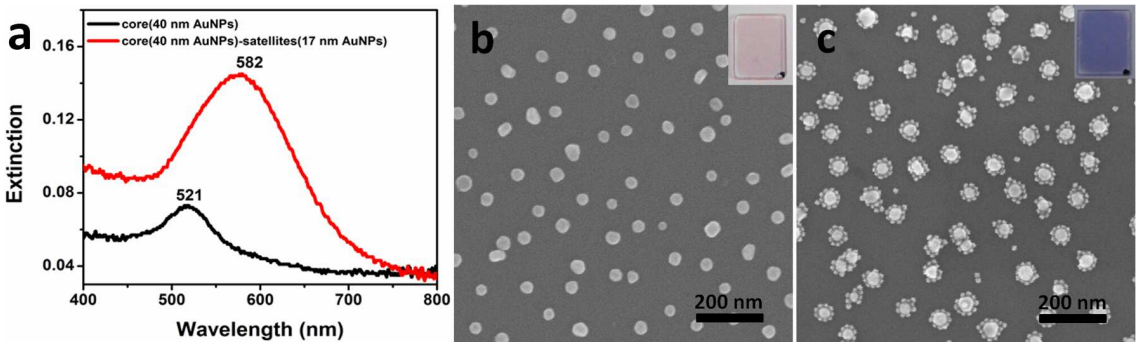

Figure 1. (a) Extiction spectra of individual Au core NPs and the as-assembled core-satellite nanostructure on the quartz substrate. SEM micrographs of (b) individual Au core NPs on average 40 nm in diameter and (c) as-assembled core-satellite nanostructures with satellite NPs on average 17 nm in diameter around 40 nm diameter core NPs on the silicon substrate. The insets reveal the obvious color difference in the core-satellite nanostructured assembly relative to individual core NPs on the quartz substrate.

Due to the most obvious red-shift in UV-vis spectra and relatively complete core-satellite structure, 40 nm diameter Au NPs and 17 nm diameter Au NPs were ultimately chosen as the core and satellite, respectively, in the following experiments to construct the self-assembly of core-satellite nanostructure on the substrate and to demonstrate its suitability as a sensing platform for the detection of target DNA. It should be mentioned that controlling the distance between neighboring core NPs is important to ensure high surface coverage density and enough space reserved for the subsequent assembly of satellite NPs. The surface coverage density of core NPs on the substrate was about $7.4\times10^{13}/m^2$. Moreover, the distance between core and satellite NPs, which is also an important factor affecting plasmonic coupling and the

corresponding changes of UV-vis spectra, was dependent on the length of the DNA sequence. The DNA sequence length used here was fixed in all experiments. The sensing capacity of as-fabricated core-satellite assembly was first investigated by the addition of different concentrations of target DNA as the linker, to check the effect on the structure of the assembly and the corresponding plasmonic coupling resonance peak in the UV-vis extinction spectra. As shown in Figure 2, with an increasing concentration of target DNA, an increase in both extinction intensity and peak shift was observed clearly in the initial concentration range of 1-100 nM, accompanied by visible color changes at the same time (Figure S3), whereas there was only a slight increase in extinction intensity when further increasing the concentration of target DNA from 100 nM to 1 μM (Figure 2 b and c). As we know that changes in the spectra result from plasmonic coupling resonance due to the target DNA guided self-assembly process, different concentrations of target DNA should lead to distinct self-assembled structures and consequent differences in the spectra. Hence, in order to more deeply understand the changes in the spectra, the morphologies of the self-assembled core-satellite nanostructures at the representative concentrations of target DNA were characterized by SEM, as shown in Figure 3. We found that at higher target DNA concentrations in the range of 100 nM to 1 μM, relatively complete and distinct core-satellite nanostructured assemblies were observed (Figure 3a and b), and the average number of satellites around each core was about 9±1 by SEM-derived statistical analysis. According to the diameter ratio of core and satellite NPs and the coplanar structure of assembly, the maximum number of satellites surrounding each core is thus expected to be approximately 10. Therefore, at a target DNA concentration above 100 nM, the number of satellites around each core is approaching saturation, which is also the reason why there was no significant change in the extinction spectra at the corresponding concentration. Up on further

decreasing the concentration of target DNA from 100 nM to 1 nM, uncompleted assembled morphologies of the core-satellites nanostructure gradually emerged (Figure 3c-f), and the average numbers of satellites around the core NPs decreased from 9±1 to 1±1, as shown in the statistical results of Figure S4. The plot of statistical average numbers of satellites around each core as a function of the logarithm of the target DNA concentration revealed a nearly linear relationship, as shown in Figure 3h. When further combining the analysis of extinction spectra with statistical results from SEM, an approximate linear increase in the peak shift as well as intensity ratio ($I_{core\text{-}satellite}/I_{core}$) was obtained with increasing numbers of satellites per core, as given in Figure 4, which is coincident with the previous theoretical prediction and experimental results and can be explained using generalized multiparticle Mie formalism.[30,47] Moreover, this result also confirms that the occurrence of the new plasmonic resonance peak is arose from core-satellite plasmonic coupling rather than satellite-satellite plasmonic coupling. The tandem relationship between the target concentration-dependent numbers of attached satellites and the satellite number-dependent plasmonic resonance peak shift fundamentally explained the DNA concentration-dependent spectra changes, and consequently demonstrated the functionality of this target DNA-directed self-assembly of plasmonic core-satellite nanostructured assembly on a substrate as a biosensor. Furthermore, it can be concluded that the changes in extinction intensity of the plasmonic coupling resonance peak as well as the peak shift are all useful criteria for detection when this core-satellite nanostructured assembly is used as a biosensor. In addition, a control experiment was performed at the 0 nM concentration of target DNA (Figure 3g), and the presence of almost only individual cores on the substrate demonstrated that target DNA is essential for the successful assembly of the core-satellite nanostructure. Compared to this control experiment, we observed significant peak shifts and enhanced extinction in the UV-vis spectra

with 1 nM target DNA guided assembly on the substrate, together with the existence of a few satellites surrounding core NPs in the SEM image, indicating a lower detection limit of 1 nM using this core-satellite nanostructured assembly on a substrate as a biosensor. The detection limit of 1 nM for target DNA is lower than that of some previous reports in solution-based methods, such as 8 nM in a plasmonic colorimetric biosensor constructed by dual compositions of Au NPs and graphene oxide,[47] and 3 nM of plasmonic NPs biosensor based on hairpin DNA modified Au NPs.[48] Therefore, the results of these comparisons demonstrate our substrate-based method is still advantageous in sensitivity. In addition, We performed an experiment in the presence of longer target DNA strand containing complementary sequences in the middle domain (30 bp) and multiple T sequences (42 bp in total) at the two terminal ends, and the appearing of new plasmonic resonance band in the extinction spectra of Figure S5 indicated the formation of core-satellite nanostructure assembly and demonstrated the ability of current system to detect longer DNA strands containing complementary sequences as a part of it. However, it is inevitable that the added multiple T sequences with 42 bases would increase steric hindrance largely and consequently hinder the hybridization of part of DNA strands for core-satellite nanostructured assembly, which is accountable for the relatively smaller changes in plasmonic resonance band compared with that arising from fully complementary short target.

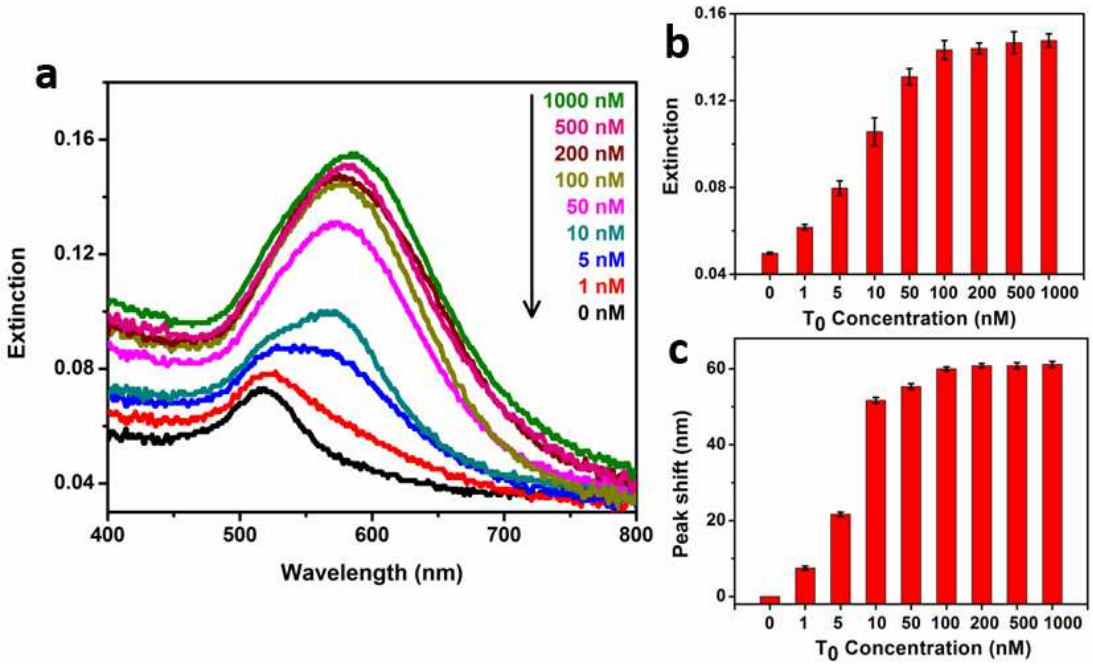

Figure 2. (a) Target DNA concentration-dependent UV-vis extinction spectral responses of the core-satellite nanostructured assembly on a quartz substrate, and histograms of the corresponding (b) extinction intensity and (c) peak shift of plasmonic coupling resonance band with respect to the concentration of target DNA.

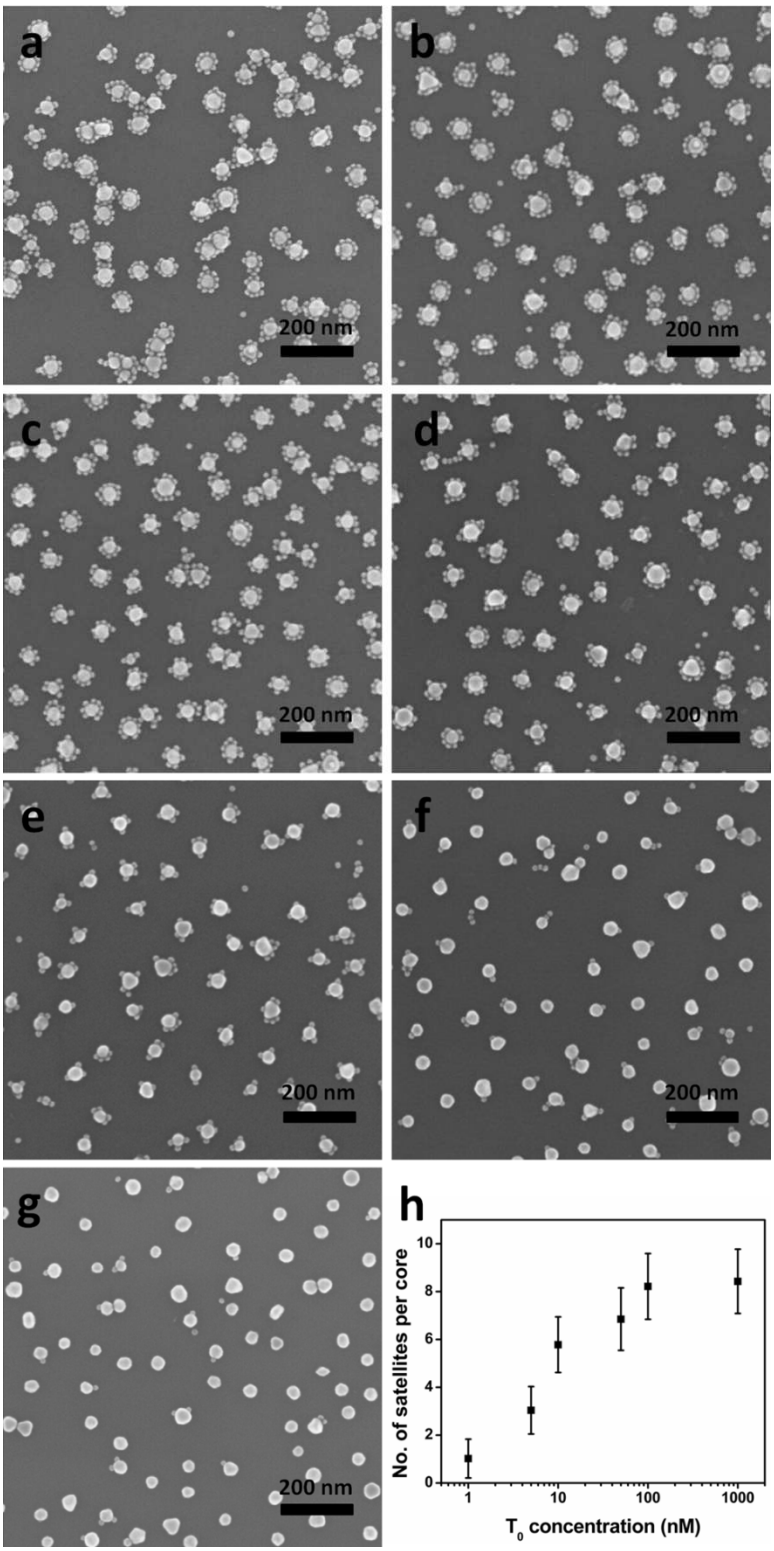

Figure 3. SEM micrographs of core-satellite nanostructured assemblies on a silicon substrate at different concentrations of target DNA: (a) 1 μM, (b) 100 nM, (c) 50 nM, (d) 10 nM, (e) 5 nM,

(f) 1 nM, (g) 0 nM. (h) Plot of statistical average numbers of satellites around per core from SEM micrographs as a function of the logarithm of target DNA concentration.

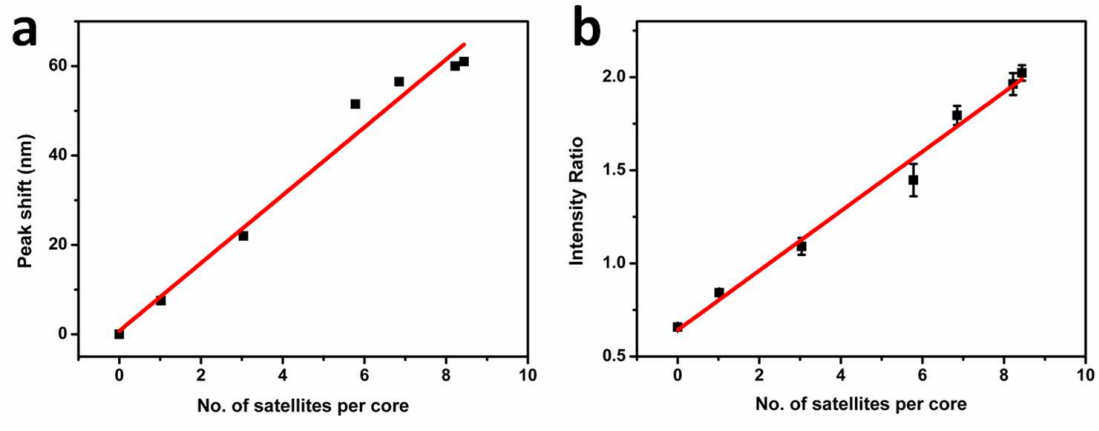

Figure 4. Plots depicting the nearly linear relationship of (a) peak shift and (b) extinction intensity ratio ($I_{core\text{-}satellite}/I_{core}$) with increasing numbers of satellites per core.

Single-nucleotide polymorphisms (SNPs) are the most abundant form of human genetic variation and the causes of many genetic diseases. Therefore, the detection of a single base mismatch is significant for disease-relevant diagnosis and treatment. It is worth mentioning that this biosensor based on core-satellite nanostructured assembly on a substrate can differentiate complementary and mismatched sequences. Figure 5 shows the distinct response of the extinction spectra toward complementary target DNA, single, two, three-base mismatched DNA and non-complementary DNA. Compared with perfectly complementary target DNA, the mismatched targets which had lower hybridization ability lead to decreased extinction intensity of the plasmonic coupling resonance peak and peak shift due to incomplete assembly. With an increasing number of mismatched bases, single, two and three-base mismatched DNA led to

93%, 86% and 76% of the extinction intensity value obtained from perfectly complementary target DNA, respectively, and obviously different peak shifts. Finally, there was no significant change in the extinction spectra in the presence of non-complementary DNA, indicating that the occurrence of the plasmonic coupling resonance peak is indeed due to the probe-target DNA hybridization guided self-assembly of the core-satellite nanostructure. We also performed the differentiation of mismatched target DNA at lower concentration of 50 nM as shown in Figure S6. Compared to the mismatched targets DNA at 100 nM concentration, lower concentration of mismatched target DNA resulted in relatively weaker plamonic resonance intensity. However, the differentiation of mismatched target DNA from complementary DNA can still be realized at current concentration based on the obvious signal difference, with single, two and three-base mismatched DNA leading to 87%, 78% and 59% of the extinction intensity value obtained from perfectly complementary target DNA, respectively, and distinctly different peak shifts. These results indicate this core-satellite assembled nanostructure system is promising in detection and differentiation of mismatched target DNA.

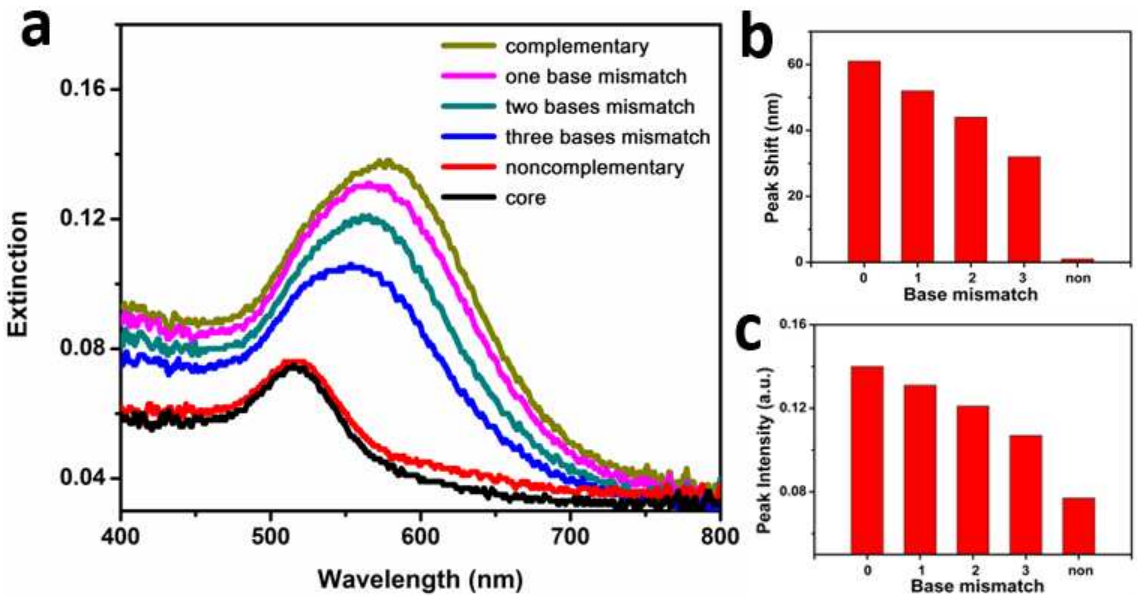

Figure 5. (a) UV-vis extinction spectra of the core-satellite nanostructured assembly in the presence of complementary target DNA, single, two, three-base mismatched DNA and non-complementary DNA, and the corresponding analysis of (b) peak shift and (c) peak intensity. The experiments were all performed at a DNA concentration of 100 nM.

The as-fabricated biosensor based on the self-assembly of a plasmonic core-satellite nanostructure displayed a highly reproducible ability regarding disassembly and reassembly due to the reversible hybridization of DNA and the immobilization of core NPs on the substrate. Figure 6 presents the microstructural changes in the core-satellite nanostructured assembly during the entire process of assembly, disassembly and reassembly. First, after the addition of 100 nM complementary target DNA, core-satellite nanostructured assemblies on the substrate were obtained due to the formation of a stable helical structure between probe DNA and target DNA, which provided the binding force between core and satellites (Figure 6b). Then, the assembled substrate was immersed in distilled water at 90^{o}C for 5 min, followed by quenching, and consequently the assembled interaction force between the cores and satellites disappeared due to DNA denaturing above the melting temperature, leading to the disassembly of the core-satellite nanostructure; only electrostatic adsorbed core NPs were left on substrate after washing thoroughly with distilled water (Figure 6c). If complementary target DNA and probe-modified satellite NPs were added to the disassembled substrate once again, reassembly of the core-satellite nanostructure occurred as a result of DNA rehybridization (Figure 6d). During the entire disassembly process, the satellite NPs could be released through the dehybridization of DNA probe capture strands with complementary target strands, while the core NPs were retained because of the electrostatic interaction between core NPs and the substrate. Hence, the

reproducible core-immobilized substrate provides a potential application for recyclable detection. Although an extremely small amount of residual satellites NPs remained on the substrate due to non-specific adsorption interactions after every cycle,[10] distinct plasmonic coupling resonance extinction was still observed and 91% of the original extinction value remained after five cycles of disassembly and reassembly, demonstrating that high cycle stability can be achieved using this reproducible core-satellite nanostructured assembly as a biosensor. The fluctuations in the differences in extinction of individual cores immobilized on the substrate are considered to be within the experimental error. Overall, this substrate-based self-assembly strategy provides an excellent approach to fabricate a reproducible biosensor.

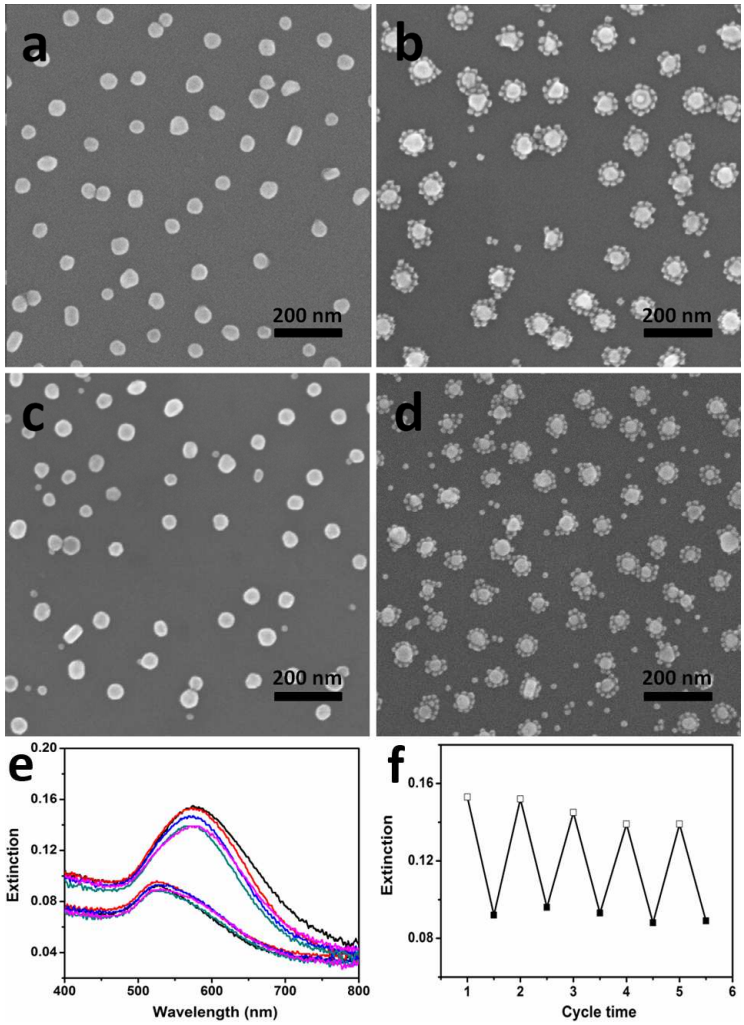

Figure 6. Characterization of repeatable assembly and disassembly of the plasmonic core-satellite nanostructure on substrates and cycling stability. SEM images of (a) individual core NPs immobilized on the silicon substrate before assembly, (b) as-prepared core-satellite nanostructured assemblies on the substrate in the first cycle after the addition of 100 nM complementary target DNA, (c) core NPs preserved on the substrate after the disassembly of core-satellite nanostructure in the first cycle, and (d) reassembled core-satellite nanostructures on the substrate in the second cycle. (e) UV-vis extinction spectra of core-satellite nanostructured assemblies on the quartz substrate during the entire process of assembly and disassembly for five cycles, and (f) the corresponding extinction peak intensity of individual core NPs (filled squares) and core-satellite nanostructured assembly (empty squares) during five cycles of disassembly and assembly.

Conclusion

In conclusion, plasmonic core-satellite nanostructured assemblies on two-dimensional substrates have been successfully constructed based on probe-target DNA hybridization directed self-assembly of satellite NPs surrounding cores immobilized on a two-dimensional substrate. Newly formed strong plasmonic coupling resonance bands were observed in the UV-vis extinction spectra of this assembly due to the close proximity between core and satellite NPs, which led to a significant red-shift and enhanced extinction compared to the LSPR band of individual core NPs on the substrate, accompanied by a visible color change. From the analysis of UV-vis extinction spectra and SEM characterization of the microstructure, we found that the extinction intensity and peak shift of the plasmonic coupling resonance band arising from the

self-assembly of core-satellite NPs due to the binding event of probe-target DNA was approximately linearly related to the number of satellites around per core, which is also a function of the logarithm of target DNA concentration. Based on this, the biosensing ability and the colorimetric detection capacity of this plasmonic core-satellite nanostructure assembly on the substrate were demonstrated at different concentrations of complementary target DNA. A detection limit of 1 nM was achieved and the differentiation of single-base mismatched DNA was also performed using this self-assembly nanostructure. One of the advantages of this substrate-based assembly as a biosensor is its reusability due to the immobilization of the core on the substrate in advance, and high cycle stability after five cycles of disassembly and reassembly was demonstrated successfully, with 91% of the original extinction value retained. We believe that this method of constructing core-satellite nanostructured assemblies on a substrate is also applicable to other plasmonic NPs with different sizes and compositions, and due to the specific recognition of the DNA probe to almost all kinds of targets, this strongly coupled plasmonic core-satellite nanostructured assembly arising from the DNA probe-target binding event can be further extended to other DNA-based detection systems for detecting biomolecules.

ASSOCIATED CONTENT

TEM micrographs and UV-vis extinction spectra of as-prepared Au NPs; UV-vis extinction spectra and SEM micrographs of as-assembled core-satellite nanostructures on substrate with fixed-sized satellite NPs of 17 nm diameter around different sized core NPs; Visible color changes of as-assembled core-satellite nanostructures on quartz substrates (1cm×1.3cm) in the presence of different concentration of target DNA; The statistical average numbers of satellites around per core from SEM micrographs at different concentrations of target DNA. Extinction

spectra of 40 nm core NPs and the as-assembled core-satellite nanostructure in the presence of longer target with added multiple T sequences. UV-vis extinction spectra of the core-satellite nanostructured assemblies in the presence of mismatched target DNA at a concentration of 50 nM. This material is available free of charge via the Internet at http://pubs.acs.org.

AUTHOR INFORMATION

Corresponding Author

E-mail: zhangyw@mail.buct.edu.cn

Notes

The authors declare no competing financial interest.

ACKNOWLEDGMENT

This work was supported by the NSFC (51302010), and the Specialized Research Fund for the Doctoral Program of Higher Education (20130010120009).

REFERENCES

(1) Liu, J. W.; Cao, Z. H.; Lu, Y. Functional Nucleic Acid Sensors. *Chem. Rev.* **2009**, *109*, 1948-1998.

(2) Du, Y.; Li, B. L.; Wang, E. K. "Fitting" Makes "Sensing" Simple: Label-Free Detection Strategies Based on Nucleic Acid Aptamers. *Acc. Chem. Res.* **2013**, *46*, 203-213.

(3) Mokhtarzadeh, A.; Dolatabadi, J. E.; Abnous, K.; de la Guardia, M.; Ramezani, M. Nanomaterial-Based Cocaine Aptasensors. *Biosens. Bioelectron.* **2015**, *68*, 95-106.

(4) Xiang, Y.; Tong, A. J.; Lu, Y. Abasic Site-Containing DNAzyme and Aptamer for Label-Free Fluorescent Detection of Pb^{2+} and Adenosine with High Sensitivity, Selectivity, and Tunable Dynamic Range. *J. Am. Chem. Soc.* **2009**, *131*, 15352-15357.

(5) He, S. J.; Song, B.; Li, D.; Zhu, C. F.; Qi, W. P.; Wen, Y. Q.; Wang, L. H; Song, S. P.; Fang, H. P.; Fan, C. H. A Graphene Nanoprobe for Rapid, Sensitive, and Multicolor Fluorescent DNA Analysis. *Adv. Funct. Mater.* **2010**, *20*, 453-459.

(6) Chang, H. X.; Tang, L. H.; Wang, Y.; Jiang, J. H.; Li, J. H. Graphene Fluorescence Resonance Energy Transfer Aptasensor for the Thrombin Detection. *Anal. Chem.* **2010**, *82*, 2341-2346.

(7) Zhang, Y. W.; Li, H. L.; Luo, Y. L.; Shi, X.; Tian, J. Q.; Sun, X. P. Poly(m-Phenylenediamine) Nanospheres and Nanorods: Selective Synthesis and Their Application for Multiplex Nucleic Acid Detection. *PloS one* **2011**, *6*, e20569.

(8) Zhang, Y. W.; Liu, S.; Sun, X. P. Mesoporous Carbon Microparticles as a Novel Fluorescent Sensing Platform for Thrombin Detection. *Biosens. Bioelectron.* **2011**, *26*, 3876-3880.

(9) Zhang, Y. W.; Sun, X. P. A Novel Fluorescent Aptasensor for Thrombin Detection: Using Poly(m-Phenylenediamine) Rods as an Effective Sensing Platform. *Chem. Commun.* **2011**, *47*, 3927-3929.

(10) Waldeisen, J. R.; Wang, T.; Ross, B. M.; Lee, L. P. Disassembly of a Core-Satellite Nanoassembled Substrate for Colorimetric Biomolecular Detection. *ACS nano* **2011**, *5*, 5383-5389.

(11) Maier, S. A. *Plasmonics: Fundamentals and Applications*. Springer US: 2007; Vol. 1, p 177-191.

(12) Halas, N. J.; Lal, S.; Chang, W. S.; Link, S.; Nordlander, P. Plasmons in Strongly Coupled Metallic Nanostructures. *Chem. Rev.* **2011**, *111*, 3913-3961.

(13) Wei, H.; Hossein Abtahi, S. M.; Vikesland, P. J. Plasmonic Colorimetric and SERS Sensors for Environmental Analysis. *Environ. Sci.: Nano* **2015**, *2*, 120-135.

(14) Underwood, S.; Mulvaney, P. Effect of the Solution Refractive Index on the Color of Gold Colloids. *Langmuir* **1994**, *10*, 3427-3430.

(15) Kelly, K. L.; Coronado, E.; Zhao, L. L.; Schatz, G. C. The Optical Properties of Metal Nanoparticles: The Influence of Size, Shape, and Dielectric Environment. *J. Phys. Chem. B* **2003**, *107*, 668-677.

(16) Su, K. H.; Wei, Q. H.; Zhang, X.; Mock, J. J.; Smith, D. R.; Schultz, S. Interparticle Coupling Effects on Plasmon Resonances of Nanogold Particles. *Nano Lett.* **2003**, *3*, 1087-1090.

(17) Hao, E.; Schatz, G. C. Electromagnetic Fields Around Silver Nanoparticles and Dimers. *J. Chem. Phys.* **2004**, *120*, 357-366.

(18) Jones, M. R.; Osberg, K. D.; Macfarlane, R. J.; Langille, M. R.; Mirkin, C. A. Templated Techniques for the Synthesis and Assembly of Plasmonic Nanostructures. *Chem. Rev.* **2011**, *111*, 3736-3827.

(19) Song, H. D.; Choi, I.; Lee, S.; Yang, Y. I.; Kang, T.; Yi, J. On-Chip Colorimetric Detection of Cu^{2+} Ions via Density-Controlled Plasmonic Core-Satellites Nanoassembly. *Anal. Chem.* **2013**, *85*, 7980-7986.

(20) Xu, W.; Xue, X. J.; Li, T. H.; Zeng, H. Q.; Liu, X. G. Ultrasensitive and Selective Colorimetric DNA Detection by Nicking Endonuclease Assisted Nanoparticle Amplification. *Angew. Chem. Int. Ed.* **2009**, *48*, 6849-6852.

(21) Xu, W.; Xie, X. J.; Li, D. W.; Yang, Z. Q.; Li, T. H.; Liu, X. G. Ultrasensitive Colorimetric DNA Detection Using a Combination of Rolling Circle Amplification and Nicking Endonuclease-Assisted Nanoparticle Amplification (NEANA). *Small* **2012**, *8*, 1846-1850.

(22) Liu, J.; Lu, Y. A Colorimetric Lead Biosensor Using DNAzyme-Directed Assembly of Gold Nanoparticles. *J. Am. Chem. Soc.* **2003**, *125*, 6642-6643.

(23) Du, J. J.; Shao, Q. ; Yin, S. Y.; Jiang, L.; Ma, J.; Chen, X. D. Colorimetric Chemodosimeter Based on Diazonium-Gold-Nanoparticle Complexes for Sulfite Ion Detection in Solution. *Small* **2012**, *8*, 3412-3416.

(24) Liu, L.; Li, S.; Liu, L.; Deng, D.; Xia, N. Simple, Sensitive and Selective Detection of Dopamine Using Dithiobis(Succinimidylpropionate)-Modified Gold Nanoparticles as Colorimetric Probes. *Analyst* **2012**, *137*, 3794-3799.

(25) Zhang, J.; Wang, L. H.; Pan, D.; Song, S. P.; Boey, F. Y.; Zhang, H.; Fan, C. H. Visual Cocaine Detection with Gold Nanoparticles and Rationally Engineered Aptamer Structures. *Small* **2008**, *4*, 1196-200.

(26) Xie, X.; Xu, W.; Liu, X. Improving Colorimetric Assays through Protein Enzyme-Assisted Gold Nanoparticle Amplification. *Acc. Chem. Res.* **2012**, *45*, 1511-1520.

(27) Elghanian, R. Selective Colorimetric Detection of Polynucleotides Based on the Distance-Dependent Optical Properties of Gold Nanoparticles. *Science* **1997**, *277*, 1078-1081.

(28) Alivisatos, A. P.; Johnsson, K. P.; Peng, X.; Wilson, T. E.; Loweth, C. J.; Bruchez, M. P., Jr.; Schultz, P. G. Organization of Nanocrystal Molecules Using DNA. *Nature* **1996**, *382*, 609-611.

(29) Yoon, J. H.; Lim, J.; Yoon, S. Controlled Assembly and Plasmonic Properties of Asymmetric Core-Satellite Nanoassemblies. *ACS nano* **2012**, *6*, 7199-7208.

(30) Gandra, N.; Abbas, A.; Tian, L.; Singamaneni, S. Plasmonic Planet-Satellite Analogues: Hierarchical Self-Assembly of Gold Nanostructures. *Nano Lett.* **2012**, *12*, 2645-2651.

(31) Liu, N.; Hentschel, M.; Weiss, T.; Alivisatos, A. P.; Giessen, H. Three-Dimensional Plasmon Rulers. *Science* **2011**, *332*, 1407-1410.

(32) Dey, P.; Zhu, S.; Thurecht, K. J.; Fredericks, P. M.; Blakey, I. Self Assembly of Plasmonic Core–Satellite Nano-Assemblies Mediated by Hyperbranched Polymer Linkers. *J. Mater. Chem. B* **2014**, *2*, 2827-2837.

(33) Liu, X. L.; Luo, C. J.; Jiang, C.; Shao, L.; Zhang, Y. W.; Shi, F. Rapid Multilayer Construction on a Non-planar Substrate by Layer-By-Layer Self-Assembly Under High Gravity. *RSC Adv.* **2014**, *4*, 59528-59534.

(34) Zhou, Y.; Cheng, M. J.; Zhu, X. Q.; Zhang, Y. J.; An, Q.; Shi, F. A Facile method for the Construction of Stable Polymer–Inorganic Nanoparticle Composite Multilayers. *J. Mater. Chem. A* **2013**, *1*, 11329-11334.

(35) Giersig, M.; Mulvaney, P. Preparation of Ordered Colloid Monolayers by Electrophoretic Deposition. *Langmuir* **1993**, *9*, 3408-3413.

(36) Bastus, N. G.; Comenge, J.; Puntes, V. Kinetically Controlled Seeded Growth Synthesis of Citrate-Stabilized Gold Nanoparticles of up to 200 nm: Size Focusing versus Ostwald Ripening. *Langmuir* **2011**, *27*, 11098-11105.

(37) Hurst, S. J.; Lytton-Jean, A. K.; Mirkin, C. A. Maximizing DNA Loading on a Range of Gold Nanoparticle Sizes. *Anal. Chem.* **2006**, *78*, 8313-8318.

(38) Jin, R. C.; Wu, G. S.; Li, Z.; Mirkin, C. A.; Schatz, G. C. What Controls the Melting Properties of DNA-Linked Gold Nanoparticle Assemblies? *J. Am. Chem. Soc.* **2003**, *125*, 1643-1654.

(39) Ding, B. Q.; Deng, Z. T.; Yan, H.; Cabrini, S.; Zuckermann, R. N.; Bokor, J. Gold Nanoparticle Self-Similar Chain Structure Organized by DNA Origami. *J. Am. Chem. Soc.* **2010**, *132*, 3248-3249.

(40) Frederix, F.; Friedt, J. M.; Choi, K. H.; Laureyn, W.; Campitelli, A.; Mondelaers, D.; Maes, G.; Borghs, G. Biosensing Based on Light Absorption of Nanoscaled Gold and Silver Particles. *Anal. Chem.* **2003**, *75*, 6894-6900.

(41) Haynes, C. L.; Van Duyne, R. P. Nanosphere Lithography: A Versatile Nanofabrication Tool for Studies of Size-Dependent Nanoparticle Optics. *J. Phys. Chem. B* **2001**, *105*, 5599-5611.

(42) Kinnan, M. K.; Chumanov, G. Plasmon Coupling in Two-Dimensional Arrays of Silver Nanoparticles: II. Effect of the Particle Size and Interparticle Distance. *J. Phys. Chem. C* **2010**, *114*, 7496-7501.

(43) Lan, X.; Chen, Z.; Liu, B. J.; Ren, B.; Henzie, J.; Wang, Q. B. DNA-Directed Gold Nanodimers with Tunable Sizes and Interparticle Distances and Their Surface Plasmonic Properties. *Small* **2013**, *9*, 2308-2315.

(44) Ross, B. M.; Waldeisen, J. R.; Wang, T.; Lee, L. P. Strategies for Nanoplasmonic Core-Satellite Biomolecular Sensors: Theory-Based Design. *Appl. Phys. Lett.* **2009**, *95*, 193112.

(45) Cha, H.; Yoon, J.; Yoon, S. Probing Quantum Plasmon Coupling Using Gold Nanoparticle Dimers with Tunable Interparticle Distances Down to the Subnanometer Range. *ACS nano* **2014**, *8*, 8554-8563.

(46) Cha, H.; Yoon, J.; Yoon, S. Gold Nanocube-Nanosphere Dimers: Preparation, Plasmon Coupling, and Surface-Enhanced Raman Scattering. *J. Phys. Chem. C* **2015**, *119*, 7873-7882.

(47) Thavanathan, J.; Huang, N. M.; Thong, K. L. Colorimetric Biosensing of Targeted Gene Sequence Using Dual Nanoparticle Platforms. *Int. J. Nanomed.* **2015**, *10*, 2711-2722.

(48) Hu, Y. L.; Zhang, L.; Zhang, Y.; Wang, B.; Wang, Y. W.; Fan, Q. L.; Huang, W.; Wang, L. H. Plasmonic Nanobiosensor Based on Hairpin DNA for Detection of Trace Oligonucleotides Biomarker in Cancers. *ACS Appl. Mater. Interfaces* **2015**, *7*, 2459-2466.

TOC graphic

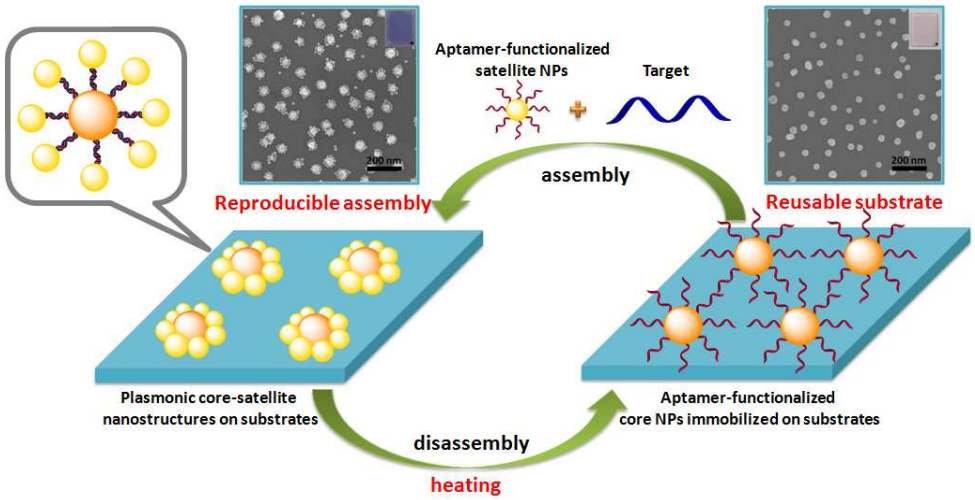
Aptamer-functionalized satellite NPs
Target
200 nm
200 nm
assembly
Reproducible assembly
Reusable substrate
Plasmonic core-satellite nanostructures on substrates
Aptamer-functionalized core NPs immobilized on substrates
disassembly
heating